

Impact of Bone Marrow Mesenchymal Stem Cells in Regeneration of the Submandibular Salivary Gland in the Albino Rat

Wafaa Yahia Alghonemy¹, Souzan Anwar Alamy¹, Amira A. R. Moawad² and Olfat Mohamed Gaballah^{1,2}

Original
Article

¹Department of Oral Biology, Faculty of Dentistry, Tanta University, Tanta, Egypt.

²Department of Oral and Maxillofacial Surgery and Diagnostic Sciences, College of Dentistry, Al-Majmaah University, Saudi Arabia

ABSTRACT

Objectives: Salivary glands are exocrine glands that function in salivary secretion and maintenance of the well-being of mouth, therefore, reduced saliva secretion has an adverse effect on oral health, general health, as well as the quality of life of the patients. Over the last decades, Mesenchymal stem cells (MSCs) have received great interest due to their potential implications in regenerative medicine.

Aim of the Study: The aim of this study was to investigate the therapeutic possible effect of locally injected BM-MSCs on regeneration of SMG after duct deligation in Albino rats using the transmission electron microscope.

Material and Methods: The study sample was consisting of 50 adult male Albino rats. Forty rats were randomly divided into two equal experimental groups; group I was subjected to extra-oral SMD ligation for two weeks and left without any treatment after duct deligation, and group II was subjected to extra-oral SMD ligation for two weeks and locally injected with BM-MCs at the time of deligation. The remaining ten rats were used for the isolation of BM-MSCs. Five rats of each group were sacrificed at day zero, just after deligation, and before any treatment to evaluate the effect of ligation and then on 3, 7 and 14 days after deligation respectively. The rats were anesthetized, and the specimens of SMG were collected and prepared for TEM investigation.

Results: TEM results of right SMGs revealed marked degenerative changes that increased in their severity from day zero to fourteen after deligation. Nonetheless, in the BM-MCs group, obvious regeneration of SMG tissues appeared at all follow-up periods commencing from day 3 to 14.

Conclusion: The extra-oral SMD ligation causes severe irreversible atrophic changes of SMG tissues. Moreover, locally injected BM-MCs offer great promise in SMG regeneration.

Received: 29 November 2021, **Accepted:** 17 May 2022

Key Words: Bone marrow mesenchymal stem cells (BM-MSCs), submandibular salivary gland duct (SMD), transmission electron microscope (TEM).

Corresponding Author: Amira A. R. Moawad, PhD, Department of Oral and Maxillofacial Surgery and Diagnostic Sciences, College of Dentistry, Al-Majmaah University 11952. Saudi Arabia, **Tel.:** 00966505366417, **E-mail:** am.deghy@gmail.com

ISSN: 1110-0559, Vol. 46, No. 3

INTRODUCTION

Over the last decade, regenerative medicine is a major part of the rapidly emerging biomedical research. It depends on numerous strategies, including the use of generated cells, biological materials as well as various growth factors to replace, repair, and improve the function of diseased or missing tissues^[1].

Stem cells are a characteristic 'unspecialized' group of cells. They are capable of dividing and self-renewing for long periods, pluripotency, and multilineage differentiation^[2,3]. These features make them different from any other type of human cell.

Stem cells are divided into three main types based on their origin. The embryonic stem cells are considered pluripotent and are derived from the inner cell mass of the embryo^[4]. The adult stem postnatal cells are found in many tissues and organs. They are considered multipotent stem cells and they can be harvested from different kinds of

tissues like bone marrow, liver, pancreas, cornea, adipose tissue, umbilical cord, amniotic fluid, brain tissue, and dental pulp^[5]. Finally, the induced pluripotent stem cells are somatic cells that are genetically reprogrammed to an embryonic stem cell-like state by being forced to express genes and factors important for maintaining the defining properties of embryonic stem cells^[6].

Mesenchymal stem cells (MSCs) are of great interest in regenerating damaged or diseased craniofacial structures as most of the craniofacial tissue is derived from mesenchymal tissues. They form a heterogeneous population of multipotent stromal cells and can be found in other tissues, including blood vessels, kidney, adipose, dermal, placental, and umbilical cord tissues^[7]. Additionally, several populations of MSCs are found in dental tissues that can be isolated from the dental pulp and the periodontal ligament and they are considered the most powerful cells for tooth engineering^[8].

Bone marrow-derived Mesenchymal Stem Cells (BM-MSCs) are fibroblast-like cells that are from the non-blood-forming fraction of bone marrow that regulates hematopoietic cell development. They have several advantages because they contain cell surface markers and can differentiate into a wide range of cells in vitro, including bone, fat, cartilage, and nerve cells^[7,9].

The submandibular salivary gland (SMG) is one of the three paired major salivary glands (SGs) in humans and rats^[10,11]. The secretory end piece of SMG is composed of a number of secretory cells and is surrounded by myoepithelial cells (MECs). Major types of acinar secretory cells are serous, forming serous acini, and mucous, forming mucous tubules. Both the human and rat SGs have the duct system composed of the main excretory ducts, (ED), striated duct (SD), and intercalated duct (ID)^[10,12]. In addition, a specialized segment of the rat's duct system is the granular convoluted tubule (GCT)^[12].

Several previous studies used extraoral ligation of submandibular ducts as a good experimental model of induced gland atrophy because it causes parasympathetic nerve damage and severe irreversible atrophic changes in gland structure^[3].

Trauma, sialadenitis, SG tumors, Sjogren's syndrome, head and neck chemotherapy, or radiotherapy are all common causes of SG atrophy. Such atrophy severely impairs salivary gland secretion, resulting in xerostomia and, as a result, oral mucositis and other pathological conditions that impair the patient's quality of life^[2,13]. The ligation of SMD has been involved in several experimental studies as a model of duct obstruction. Notably, duct ligation results in a variety of atrophic changes that vary depending on the surgical approach, location, and duration of ligation. Furthermore, these pathological changes may be reversible or irreversible^[3,14].

The aim of this study was to investigate the therapeutic possible effect of locally injected BM-MSCs on regeneration of SMG after duct deligation in albino rats using a transmission electron microscope.

MATERIALS AND METHODS

A total of 50 adult male albino rats with an average weight of 200-250 grams were used in this study. 10 rats were used for isolation BM-MSCs. 40 rats were subjected to extraoral right SMD ligation for two weeks and deligation after two weeks. Afterward, the animals were randomly divided into untreated control group (GI) and experimental group (GII) each containing 20 rats. The GI was subjected to intra-glandular (IG) injection with 1 ml sterile physiological saline at the time of deligation to control the influence of injection stress of anesthesia and left without treatment after deligation. While the GII was treated with (IG) injection of isolated BM-MSCs solution once at the time of deligation. (Each rat has received 1×10^6 BM-MSCs suspension per 250 gm of body weight)^[15].

This study was designed in accordance with the guidelines for the responsible use of animals in research as a part of the scientific research ethics recommendation of the ethical committee at the Faculty of Dentistry, Tanta University.

Duct Ligation: The animals were anesthetized through intraperitoneal injection with Ketamine hydrochloride 10 % with xylazine hydrochloride 2 at a dosage of 0.06 ml/g body weight & 0.03 ml/g body weight, respectively,^[16] A small skin incision was done on the midline of the ventral surface of the rat neck and right SMG was exposed. Then, SMD was ligated less than 5 mm anterior to the hilum of the gland with an 8/0 suture and the incision was sutured with a 4/0 absorbable silk suture^[15,17-19].

Duct deligation: After 2 weeks the rats were anesthetized as before then the right SMD was deligated by removing the suture obstructing SMD carefully without causing any damage, then the incision was sutured with 4/0 absorbable silk suture and the rats were allowed to recover from anesthesia^[18,19].

Culture, harvesting, and characterization of BMSCs

The bone marrow of both femurs of the 10 rats was flushed in a complete culture medium after their euthanization with an overdose of anesthesia. The Complete medium was composed of DMEM-LG, 10% FBS, 1% L-Glutamine & 1% pen/strept (Lonza Bioproducts, Belgium). Then the flushed bone marrow was centrifuged at 1200 RPM for 8 min. The pellet was re-suspended in 5% complete media and then transferred to a standard tissue culture flask for incubation in the CO₂ incubator at temp 37°C. After 3 days, the medium was discarded, and the adherent cells were washed with PBS and a fresh complete medium was inserted in the flask. Culture medium change was done twice weekly till 80% confluence. Cells in the 3rd passage were harvested by trypsinization and counted using an improved Neubauer Hemocytometer, (Figure 1)^[20].

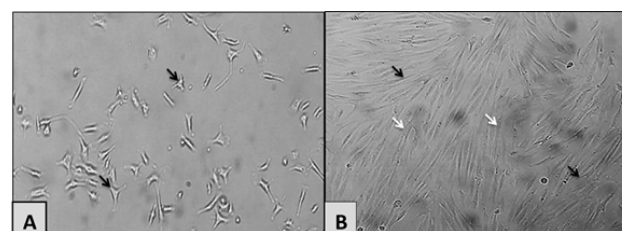


Fig. 1: A photomicrograph shows (A) isolated MSCs after 1 week, the cells display fibroblast-like morphology (black arrows), (B) A photomicrograph shows isolated MSCs of third passage, the cells display fibroblast-like morphology: large nuclei (white arrows) and long thin processes (black arrows) (Inverted microscope, X100).

The adherent property of BM-MSCs to uncoated tissue culture dishes, their typical spindle-shaped or fibroblast-like morphology when examined under an inverted microscope, and further characterization using flow cytometer analysis were used to identify them^[21,22].

The cells were stained with different fluorescently labeled monoclonal antibodies (mAb). MSCs were characterized for CD44, CD90 as positive markers, in addition to CD34 as a negative marker (Abcam, UK). Flow cytometer analysis showed that 98.75% and 92.42% of BM-MSCs were positive to CD90 and CD105, respectively, while only 1.36% were positive for CD34 which is considered as a negative result, (Figure 2)^[20]. Five rats of each group were sacrificed with an overdose of anesthesia at day zero, and then after 3, 7, and 14 days^[15,18,23] after deligation respectively. Right SMG specimens were dissected carefully and then prepared for a transmission electron microscope to investigate the ultrastructural cellular changes in both groups.

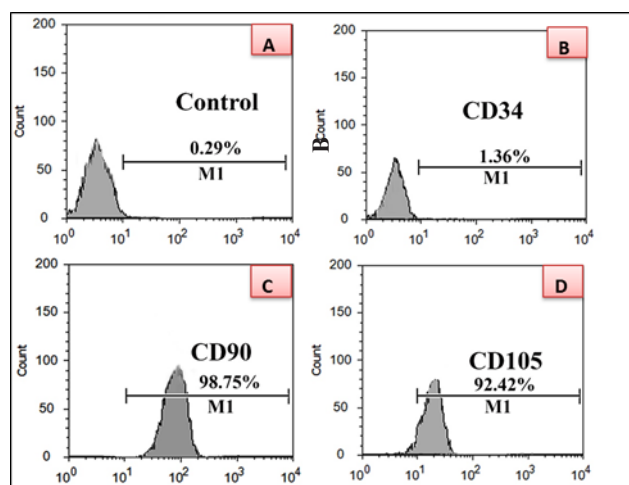


Fig. 2: A Histogram depicts characterization of BM-MSCs by flow cytometer analysis, A, Isotype control; B, BM-MSCs negative to CD34; C&D, BM-MSCs positive to CD90 & CD105.

RESULTS

Untreated control group

Rats in this group were subjected to SMD ligation of right SMG for two weeks and were left without any treatment after deligation.

Treated group

Rats in this group were subjected to SMD ligation of the right SMG for two weeks and they were received BM-MSCs once at the time of deligation

At day zero

The acini of SMG in the untreated and treated groups were seromucous and they exhibited some degenerative changes. The nerve axon appeared unmyelinated and showed great degeneration of nerve fibres that resulted in the appearance of empty endoneurial tubes. Surprisingly, a thin myelin sheath was visible inside the degenerated nerve. Schwann cell with a heterochromatic nucleus and condensed cytoplasm was depicted near a large blood vessel, (Figure 3 A,B,C,D).

At day three

TEM examination of the untreated group showed that SMD tissues still depicted some degenerative changes. Unmyelinated nerve axon appeared near large blood vessel and its nerve bundles showed endoneurial fibrosis. The nerve bundles were wrapped by Schwann cell (SC) cytoplasm that contains swollen mitochondria. (Figure 4 A,B,C,D), while the treated group showed that the acinar cells have depicted euchromatic nuclei that might be binucleated and a few secretory granules near the acinus lumen, also there were large cytoplasmic vacuoles were appeared in the acinar cells and RER appeared normal and sometimes dilated or disorganized. Unmyelinated nerve axon depicted degeneration of endoneurial membrane of some nerve bundles. Also, there was the loss of continuity of the SC plasma membrane and its mitochondria appeared atrophied (Figure 4 E,F,G,H).

At day seven

The acinar cells in the untreated group showed impaired cell organelles, pyknotic nuclei, small and large cytoplasmic vacuoles, and disorganized RER. The striated duct showed loss of basal striations in some areas and cytoplasmic vacuoles. Destructed nerve axon with great degeneration of the bundles and endoneurial membrane could be represented. Schwann cell depicted loss plasma membrane continuity and its cytoplasm contained atrophied mitochondria, (Figure 5 A,B,C,D), While the treated group showed acinar cells with active nuclei, almost normal RER and mitochondria, few cytoplasmic vacuolization, moderately widened intercellular space. Cells of granular convoluted tubules (GCT) depicted euchromatic nuclei, some cells depicted clear granular accumulation with different sizes, cytoplasmic vacuolization, almost normal intercellular junction, and intact basal lamina Moreover, striated duct (SD) contained euchromatic nuclei, few pyknotic nuclei, few cytoplasmic vacuolizations, almost normal intercellular junction and the basal lamina, small electron-dense secretory granules, and mitochondria at the basal area. Unmyelinated nerve axon showed discontinuity of endoneurial membrane, but Schwann cell (SC) membrane appeared intact and surrounded the nerve axon, (Figure 5 E,F,G,H).

At day fourteen The acinar in the untreated group showed pyknotic nuclei, fragmented RER, and small scattered mitochondria were seen. Striated duct cells with pyknotic and heterochromatic nuclei, small scattered mitochondria, large cytoplasmic vacuoles, and little basal striations were clearly seen. The nerve axon in the CT stroma appeared shrunken and showed great degeneration of the bundles and in the remaining endoneurial membrane. Schwann cell (SC) showed loss of its plasma membrane continuity and condensed cytoplasm, (Figure 6 A,B,C,D), While The acinus cells in the treated group appeared loaded with secretory granules near a large lumen. Also, they contained basally located heterochromatic nuclei. The ducts depicted an almost normal structure. The SD lined with columnar

cells They contained basal euchromatic nuclei, basal striations, and electron-dense secretory granules near the lumen. Unmyelinated nerve axon located near large blood vessel appeared with almost normal structure. Each nerve

bundle was wrapped by cytoplasmic processes of SC. Also, the nerve appeared enveloped with an intact plasma membrane of SC fig. (Figure 6 E,F,G,H)

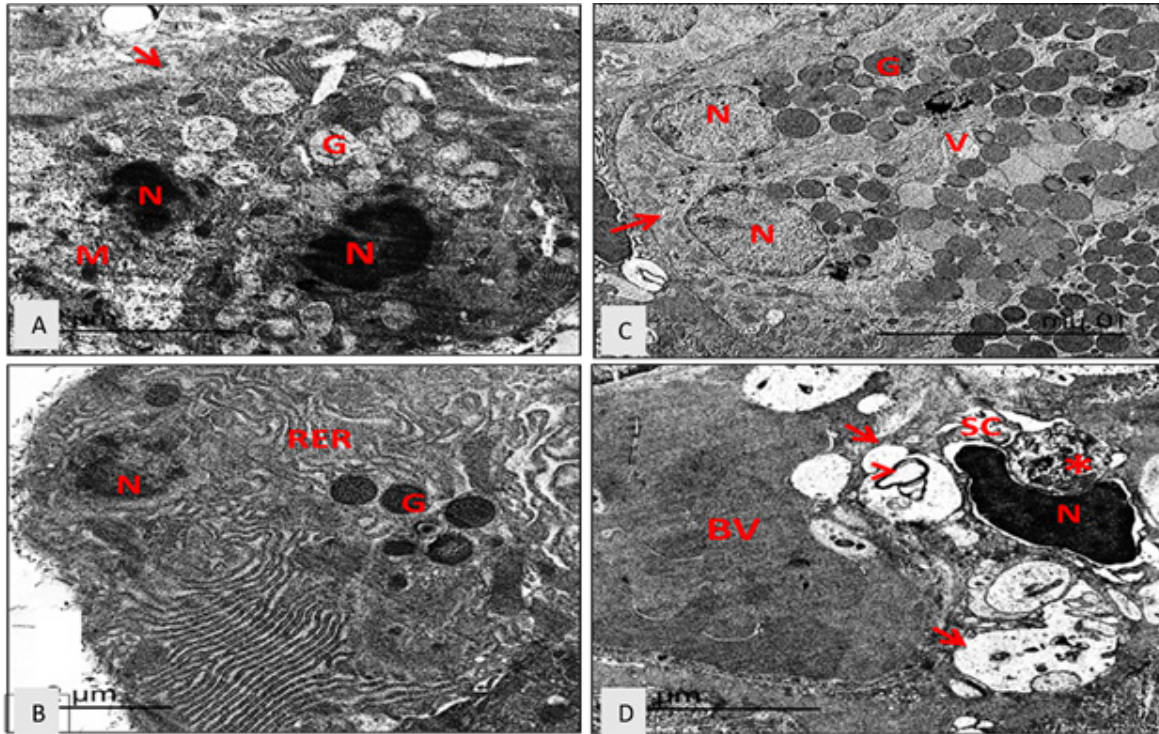


Fig. 3: A TEM micrograph at day zero after deligation of the untreated control group reveals: (A) A sero-mucous acinar cell with nuclear shrinkage with chromatin condensation (N), and some secretory granules (G) degenerated mitochondria (M) Also, there is a discontinuity in the cell membrane (arrow). (B) Electron-dense secretory granules (G), RER with few alterations (arrow). (C) cells of the striated duct with euchromatic nuclei (N), less prominent basal striations (arrow), electron-dense secretory granules (G), cytoplasmic vacuoles (V) can be distinguished. (D) T.S. in an unmyelinated nerve axon and its SC near large blood vessel (BV). The nerve shows great degeneration of nerve fibers leaving the corresponding endoneurial tubes (arrows). Schwann cell appears to contain a heterochromatic nucleus (N) and condensed cytoplasm (*). Notice thin myelin sheath inside the degenerated nerve (arrowhead). (Mic. Mag. A& C X 800 and B & D X 1200).

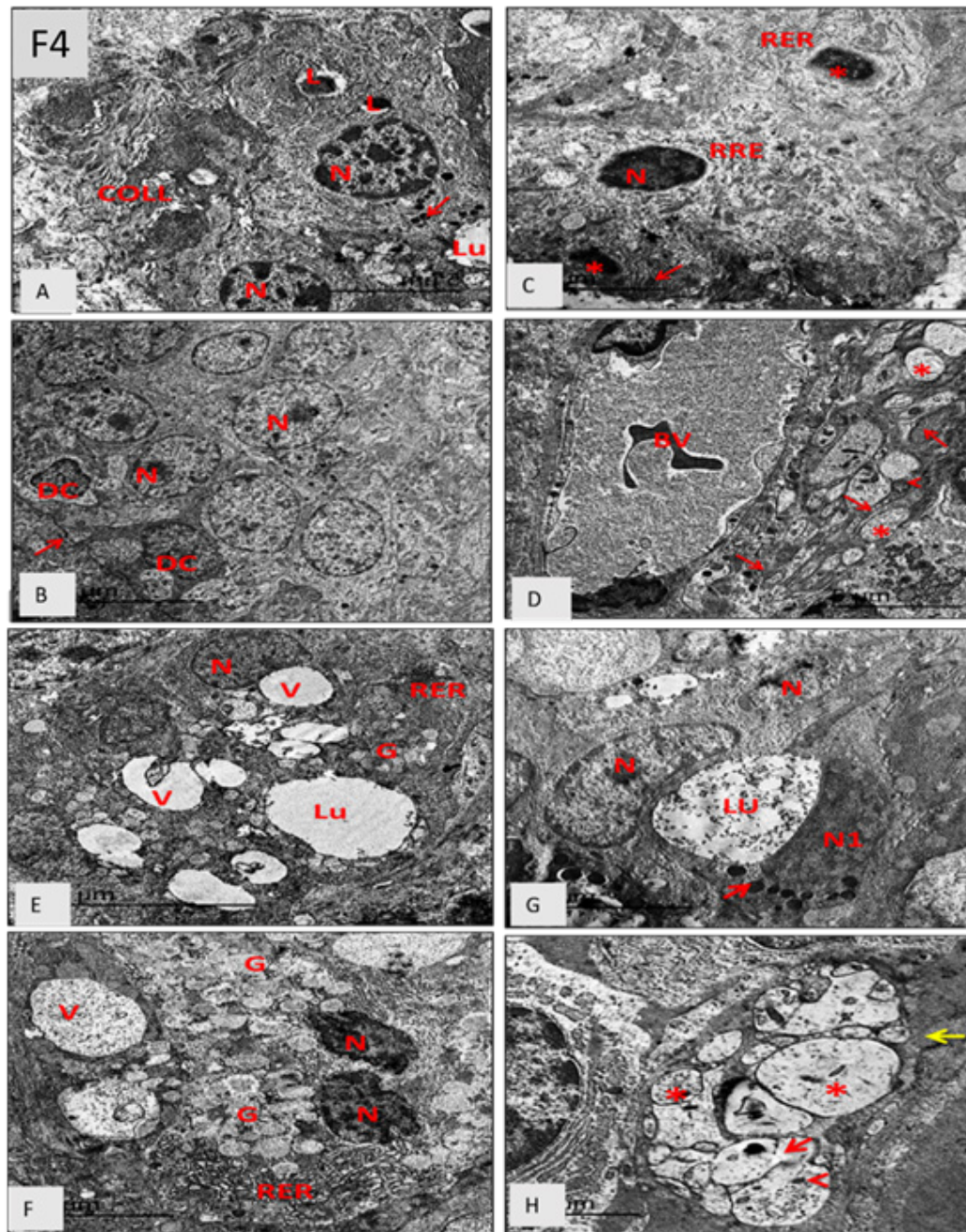


Fig. 4: A TEM micrograph: three days after deligation of the untreated control group reveals: (A) The acini appear with rounded basally located nucleus (N) and few electron-dense granules (arrow). There are lysosomal bodies (L) There is an increased amount of collagen fibres (Coll) in CT septa. (B) Intra-lobular duct lined with stratified epithelium containing euchromatic nuclei (N), and intact basal lamina and (arrow). Notice, dendritic cells (DC) are seen at the basal region of duct epithelium. (C) striated duct cells with pyknotic nuclei (*) and heterochromatic nucleus (N), fragmented RER and partial loss of basal striations with few abnormal mitochondria (arrow). (D) T.S. in unmyelinated nerve axon near large blood vessel (BV). The nerve bundles (*) show endoneurial fibrosis (arrows). Notice abnormal mitochondria (arrowhead) in the SC cytoplasm. The treated group reveals, (E) An acinar cells with euchromatic nuclei (N) and a few electron-lucent secretory granules (G) near the acinus lumen (Lu). Also, there are large cytoplasmic vacuoles (V) and a few disorganized RER. (F) Binucleated (N) acinar cell with condensed electron-lucent secretory granules (G). Also, there are large cytoplasmic vacuoles (V) and dilated disorganized RER. (G) The intercalated duct that is lined with cuboidal cells with euchromatic (N) and heterochromatic nuclei(N1) around a large lumen (LU). There are some dense secretory granules (arrow) in the duct cells. (H) T.S. in an unmyelinated nerve axon displaying degeneration of an endoneurial membrane (red arrow) of some nerve bundles (*). Also, there is a loss of the continuity of the SC plasma membrane (yellow arrow) and its mitochondria (arrowhead) appear atrophied. (Mic. Mag. A & C and B & D X 1000), (E & G X 1200 and F & H X 2000).

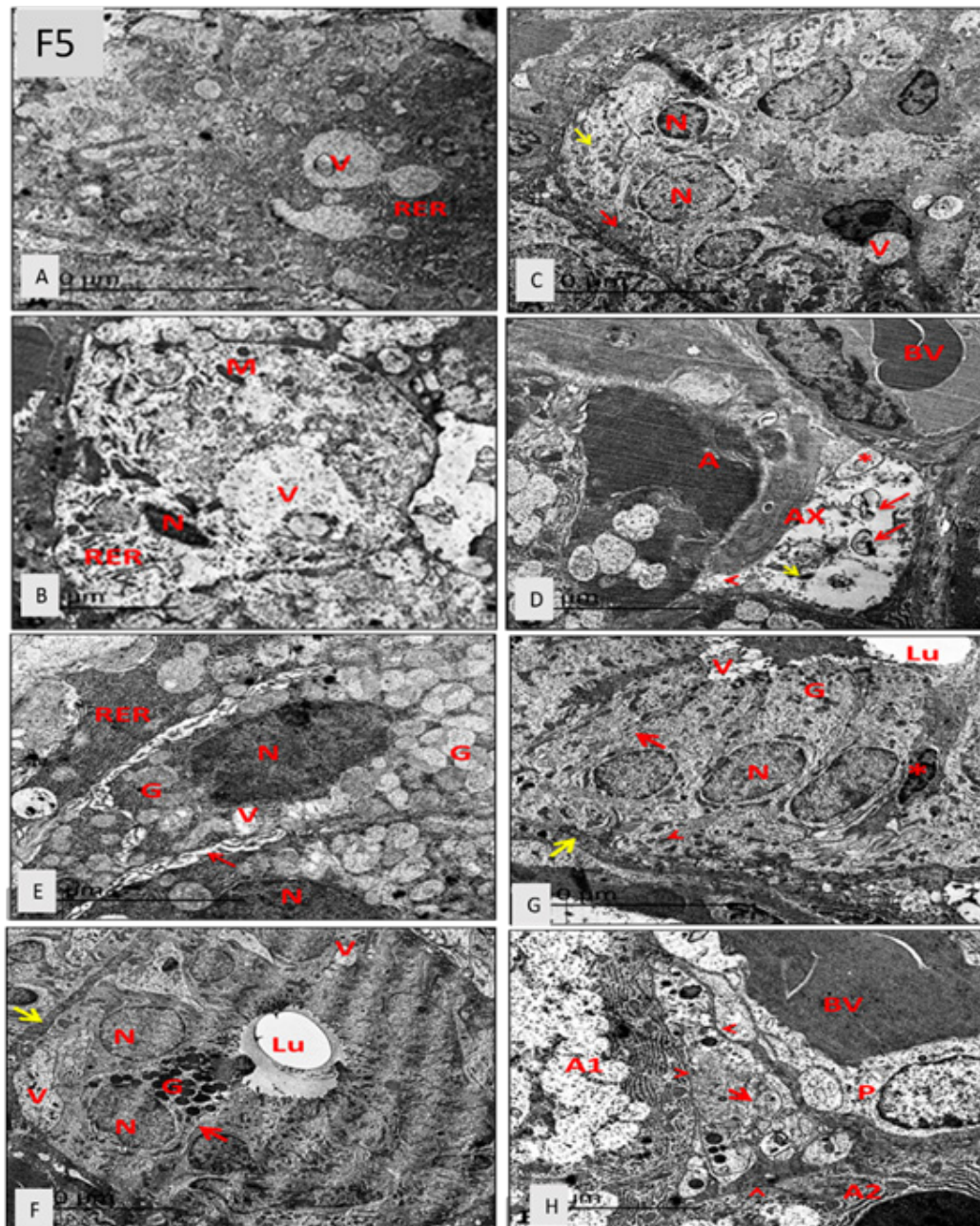


Fig. 5: A TEM micrograph, seven days after deligation of the untreated control group reveals: (A) A destructed acinar cells with cytoplasmic vacuoles (V) and impaired cell organelles. Disorganization of RER. (B) acinar cell with pyknotic nucleus (N) fragmented RER, large cytoplasmic vacuole and small scattered mitochondria (M). (C) Cells of SD with euchromatic nuclei (N) and basal striations (red arrow) in a small area and loss of the striation in another area (yellow arrow). Cytoplasmic vacuoles (V) (D) T.S. of destructed nerve axon (AX) lying in between seromucous acinus (A) and large blood vessel (BV). The nerve shows a great degeneration of the bundles and an endoneurial membrane (red arrows), only one nerve bundle (*) with intact an endoneurial membrane can be distinguished. The Schwann cell shows a loss of the plasma membrane continuity (arrowhead) and atrophied mitochondria (M). The treated group reveals, (E) A seromucous acinar with Nucleus (N) well-organized RER, few cytoplasmic vacuolization (V), moderately widened intercellular space (arrow). Also, the cell is loaded with less electron-dense secretory granules (G) which coalesce with each other. (F) the cells of GCT contain euchromatic nuclei (N), some cells depict clear electron-dense granular accumulation (G) and cytoplasmic vacuolization (V). Also, the almost normal intercellular junction (red arrow) and intact basal lamina (yellow arrow). (G) the cells of the SD contain euchromatic nuclei (N), few pyknotic nuclei (*), few cytoplasmic vacuolization (V), almost normal intercellular junction (red arrow) and basal lamina (yellow arrow), small electron-dense secretory granules (G) and mitochondria (arrowheads) at the basal area. (H) T.S. in an unmyelinated nerve axon in between seromucous acini (A1, A2) and BV with a normal pericyte (P). The nerve axons still show discontinuity of the endoneurial membrane (arrow) but the SC plasma membrane appears intact and surrounds the nerve axon (arrowheads). (Mic. Mag. A&C X 600 and B &DX 1200), (E& G X 800 and F&H X 1200).

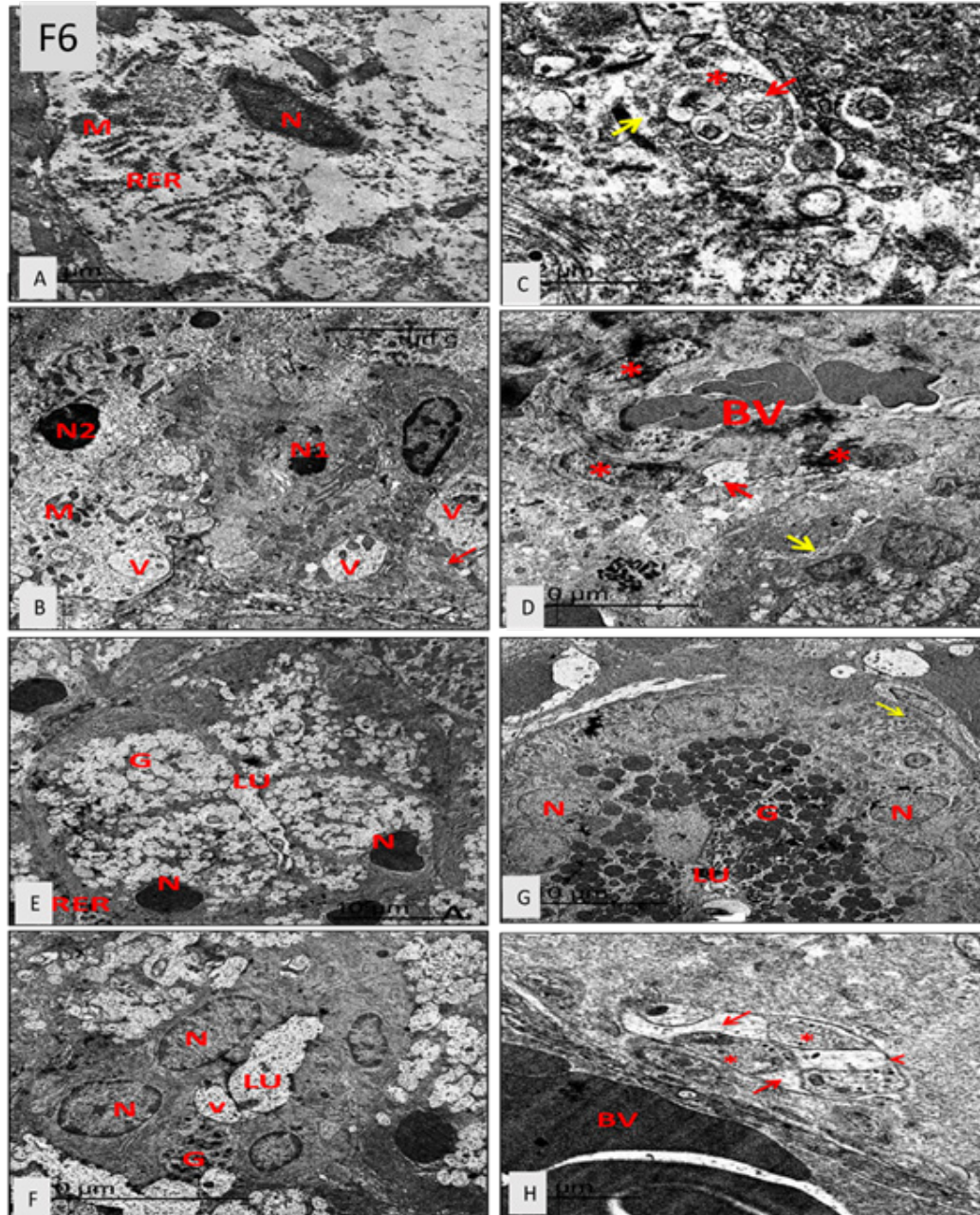


Fig. 6: A TEM micrograph, fourteen days after deligation of the untreated control group reveals: (A) An acinar cell with pyknotic nucleus (N) fragmented RER and scattered abnormal mitochondria (M). (B) Striated duct cells with pyknotic nuclei (N1), heterochromatic nucleus (N2), small scattered mitochondria (M) large cytoplasmic vacuoles (V), and few basal striations (arrow). (C) T.S. of a shrunken nerve axon in CT stroma. The nerve shows a great degeneration of the bundles and degeneration in the remaining endoneurial membrane (red arrow). Schwann cell cytoplasm appears condensed (*) and there is a loss of continuity of its plasma membrane (yellow arrow). (D) The CT contains a large blood vessel (BV) with rupture in a small part of its wall (red arrow) and intact endothelial cells in another part (*). Notice, widening of the basal lamina of acinar cells (yellow arrow). The treated group reveals, (E) a seromucous acinus in which the cells appear loaded with secretory granules (G), containing basally located heterochromatic nuclei (N), and almost normal RER. The cells surround a large lumen (LU). (F) an almost normal intercalated duct is lined with cuboidal cells that have euchromatic nuclei (N) around a large lumen (LU), the duct cells contain a few cytoplasmic vacuolization (V) and an electron-dense secretory granules (G). (G) an almost normal SD is lined with columnar cells that have basal euchromatic nuclei (N) and basal striations (yellow arrow) electron-dense secretory granules (G) near the lumen (Lu). (H) T.S. in an unmyelinated nerve axon near large BV. Each nerve bundle (*) appears wrapped by cytoplasmic processes of SC (arrows). Also, the nerve appears enveloped with an intact plasma membrane of SC (arrowhead). (Mic. Mag. A & C X 2500 and B&D X 600). (E X 500 and F X 2000).

DISCUSSION

It has long been necessary to develop a novel conceptual therapy for the regeneration of the atrophied salivary gland. Recently, researchers have attempted to implement novel therapeutic strategies such as stem cell or gene therapy, as well as bioengineering approaches, for the functional regeneration of salivary glands^[24].

The multipotent adult or post-natal mesenchymal stem cells (MSCs) have received more interest in the last two decades because of their immunomodulatory properties^[25,26]. Besides, the higher differentiation potential could provide additional benefits during tissue regeneration.

This study has been conducted to demonstrate the role of BM-MSCs in the regeneration of SMG atrophy following extra oral duct ligation of albino rats. Extraoral SMD ligation has been used as a model of duct obstruction mimicking the condition associated with diseases. Previous studies found that when the chorda tympani nerve was included in the duct ligation, there was irreversible SMG atrophy compared to nerve exclusion because the parasympathetic nerve has an atrophic effect on SGs^[3,27]. To evaluate the tissue changes in acini, ducts, blood vessels, nerve and SCs, we studied SMG tissues under TEM that enables the resolution and visualization in detail^[28].

In the current study, we isolated and characterized the BMSCs lines from rat bone marrow. For proliferation and differentiation of BMSC cells, DMEM-based media has been used that contains L-glutamine as it has greater proliferation in various cell types and this had been attributed to the greater stability of the L-glutamine. Also, following the protocol of Aly *et al.*^[16], we used the third passage not more with 80% confluence to achieve the best results as cells could lose their multipotential ability with increasing the passage number due to rapid aging to MSCs and loss of surface receptors as a result of the increased rate of telomere loss^[29,30].

The heterogeneity of MSC surface receptor expression emphasizes the critical importance of MSC characterization. In the current study, we used flow cytometric analysis of expressed surface antigens, which is reproducible, fast, and reliable, and allows us to characterize MSCs regardless of whether trypsin was used to remove the cells from the substrate^[31]. MSCs have been reported to be uniformly positive for CD44 and CD90 and negative for CD34^[32].

In the current study, we preferred to use the IG delivery route rather than systematic IV injection. As IG delivery route is less time-consuming and required a quarter of IV dosage with the concentrated number of cells that might be stuck in the other tissues in case of IV injection^[31]. We locally injected a million of BM-MSCs into the macroscopic center of SMG at the time of deligation following the protocol of Schwarz *et al.*^[15].

The TEM results of ligated right SMGs of the untreated control group revealed marked degenerative changes that

persisted on all follow-up periods. The severity of these changes was increased gradually from day zero to 14. This result was in agreement with several studies which declared that there was irreversible SMG atrophy following extra oral SMD ligation^[18,27].

It is worth mentioning that, ultrastructural examination in the present study revealed that right SMGs of control rats exhibited signs of cell injury and degeneration. The mitochondria exhibited swelling, atrophy, or complete disappearance in SMG acinar and ductal cells and a marked decrease in number within the basal part of SD with loss of basal striations at the all-time intervals after deligation. These results were in accordance with Shiba *et al.* who found that after 7 days of SMG ligation, basal infoldings of SD disappeared and the number of mitochondria was decreased. They referred this change as regressive atrophy, caused by the reduced enzymatic activity and the pressure of the excreted substance, that occurred in the epithelium of the dilated duct^[33].

The discontinuity of the plasma cell membrane was the other degenerative change that was visible in TEM examination at all follow-up times. Kroemer *et al.*^[34] explained that the cell was dead and could be regarded as the point-of-no-return when the epithelial cell's plasma membrane had lost its integrity.

At all follow-up periods, dilated and fragmented RER was found in both acinar and ductal cells of the right SMGs of positive control rats. This observation was coordinated with another that showed RER disintegration on acinar cells on the first day of ligation and being ingested by autophagic vacuoles that primarily contained RER^[35]. Tamarin^[36] found that after 30 days of SMD deligation, dramatic microscopical changes in cell structures were observed, including intralaminar dilatation of RER in duct cells. He interpreted the dilatation of the RER followed by its disintegration, as an eventual incidence of cell death. Moreover, we noticed that there were lysosomal bodies inside the seromucous acinar cells on day 3 after duct deligation of the right SMG of the control group. This result was consistent with that depicted by previous studies at 24 hours and 3 days after ligation^[33,37] Importantly, lysosomes play role in apoptosis progression and terminal steps of autophagy as Ivanova *et al.*^[38] confirmed. that lysosomes contained proteases that were released into the cytosol and cause apoptosis progression.

In addition, the ultrastructural examination of the current study revealed that the right SMGs of the control group demonstrated different types of nuclear modifications. The condensed pyknotic nuclei appeared within some acinar and ductal cells at all follow-up periods. This finding was similar to that of Walker and Gobé^[35] who noticed nuclear pyknosis after ED ligation of the parotid gland for 5 days. Lodish *et al.*^[39] reported that nuclear pyknosis is one of the multiple signs of programmed cell death which was consisted of nuclear fragmentation, clumping of chromatin against the nuclear membrane, overall cell shrinkage

resulting in enlargement of the intercellular space, and cell fragmentation to form groups of rounded eosinophilic and basophilic of apoptotic bodies. Interestingly, dendritic cells were seen at the basal region of the intralobular duct epithelium in the right SMG of the control group at day 3 after duct deligation. Stasulis and Hand^[40] reported that DCs in SG duct epithelium was monocyte lineage cells and their presence in SGs might be exposed to antigens and that DCs might participate in local immune responses.

Moreover, signs of nerve and SCs degenerations appeared with TEM examination in all follow-up periods of the right SMG of the control group. The nerve axon appeared shrunken and showed great degeneration of the nerve bundles and endoneurial membrane. SCs showed signs of cell injury and degeneration as condensed cytoplasm with closed face nucleus at day 3 after deligation. The mitochondria exhibited swelling and atrophy at days 3 and 7 after deligation respectively. Also, they showed loss of plasma membrane continuity at day 14 after deligation. These findings were similar to those reported by Harrison et al.^[41], who found that after SMD ligation with the inclusion of the chorda tympani nerve in feline cats on day 5, nerve axons degenerated and the remaining ones were surrounded by a relatively increased amount of condensed cytoplasm of SCs.

The TEM results of right SMGs in the stem cell group revealed obvious regeneration of SMG tissues at all follow-up periods ranging from day 3 to 14 after duct deligation, as the tissue appeared with almost normal microscopical structures. SMG tissue exhibited acinar and ductal cells with open-faced nuclei, nearly normal cell organelles and intercellular junctions, intact basal lamina, and SD basal striations. Nonetheless, few signs of degeneration as cytoplasmic vacuolisations were still depicted. Also, signs of regenerations as binucleation of acinar cells and proliferated blood vessels in close contact with the acini and ducts also appeared. Moreover, nerve axon and SCs showed regeneration with few signs of degeneration as degeneration of endoneurial membrane and loss of continuity of SC plasma membrane especially at the early days after treatment. Outstandingly, the presence of binucleation might indicate an increase in cellular activity that occurs during cell reproduction and regeneration^[42]. Denny and Denny^[43] found that acinar and ductal cells of SMG of mouse exhibited binucleation and regenerate continually which is the regeneration manifestations.

Likewise, nerve axon and SCs showed almost normal appearances under TEM. This result is in agreement with Caddick et al.^[44] who found that differentiated BM-MSCs enhanced neurite outgrowth when they co-cultured with sensory neurons to a level superior or equivalent to that produced by SCs. On the other hand, Ke et al.^[45] found that BM-MSCs significantly improve the function of the sciatic nerve, and led to increased expression of netrin-1, BDNF, and NGF at day 7 and 14 after injection. Moreover, earlier studies found that MSCs can differentiate into neuronal phenotypes including astrocytes, oligodendrocytes, microglia and neurons^[46,47].

MSCs are responsible for the secretion of cytokines, which can act via one of three mechanisms: autocrine, paracrine, or endocrine. It was discovered that paracrine signaling, rather than direct cell incorporation, may be responsible for the effects of BM cell therapy in ischemic injury^[48]. Thus, the cytokines secreted during MSC therapy are known as paracrine factors, and they have been shown to be up-regulated following BM-MSCs soup injection in previous studies^[49]. These factors are well known to promote angiogenesis and neovascularization^[48]. Tran et al.^[49] found that BM soup injection up-regulated expression of tissue remodeling, repair, and regenerative factors as MMP-2, CyclinD1, BMP7, EGF, and NGF, and restored morphology of irradiation-damaged SMGs of mice. Also, Fang et al.^[50] found that BM soup up-regulated expression of MMP-8, MMP-9, FGF-1, OPN and SDF-1, some anti-angiogenic factors (PF4 and CD26), and two cytokines, IL-1 and IL-1ra, and re-established SGs morphology of irradiation-damaged SGs

Worth mentioning, the factors that might explain our positive results and accelerate the regeneration of the SMSG after IG injection of BM-MSCs are BM-MSCs differentiation into fibroblasts and trans-differentiation into acinar and ductal cells^[51-54], MSCs are responsible for the secretion of cytokines that has paracrine action which promotes angiogenesis and neovascularization, finally, inhibition of both apoptosis and inflammation is another important role of MSCs^[55,56].

CONCLUSION

Finally, our study clarified that BM-MSCs are histologically effective in the regeneration of SMGs after induction of severe atrophy via parasympathetic denervation. Hence, BM-MSCs therapy can be a promising therapeutic effect on the regeneration of SMGs. However, further clinical and histological studies with different parameters should be performed to evaluate the effect of the long-term treatment using BM-MSCs as a therapeutic agent.

CONFLICT OF INTERESTS

There are no conflicts of interest.

REFERENCES

1. Bajaj P, Schweller RM, Khademhosseini A, West JL, Bashir R. 3D bio fabrication strategies for tissue engineering and regenerative medicine. *Annu Rev Biomed Eng* 2014; 16:247–276.
2. Grisius MM. Salivary gland dysfunction: a review of systemic therapies. *Oral Surgery, Oral Med Oral Pathol Oral Radiol Endod.* 2001; 92:156–162.
3. Osailan SM, Proctor GB, McGurk M, Paterson KL. Intraoral duct ligation without the inclusion of the parasympathetic nerve supply induces rat submandibular gland atrophy. *Int J Exp Pathol.* 2006;87(1):41–48.

4. Thomson J, Itskovitz-eldor J, Shapiro S, Waknitz M, Swiergiel J, Marshall V, et al. Embryonic Stem Cell Lines Derived from Human Blastocysts. *Science*. 1998; 282:1145–1148.
5. Shete M, Byakodi R, Kshar A, Paranjpe A. Stem Cell Therapy in Dentistry: An Overview. *IJSS Case Reports & Reviews*. 2015; 1(8):50–54.
6. Takahashi K, Yamanaka S. Induction of pluripotent stem cells from mouse embryonic and adult fibroblast cultures by defined factors. *Cell*. 2006; 126(4):663–676.
7. Pittenger MF, Mackay AM, Beck SC, Jaiswal RK, Douglas R, Mosca JD, et al. Multilineage potential of adult human mesenchymal stem cells. *Science*. 1999; 284(5411):143–147.
8. Lymperti S, Ligoudistianou C, Taraslia V, Kontakiotis E, Anastasiadou E. Dental Stem Cells and their Applications in Dental Tissue Engineering. *Open Dent J*. 2013; 7(1):76–81.
9. Barry F, Murphy J. Mesenchymal stem cells: Clinical applications and biological characterization. *Int J Biochem Cell Biol*. 2004; 36(4):568–584.
10. Nanci A. Ten cate's oral histology: development, structure, and function. 8th ed. *Salivary Glands*: Mosby: Elsevier Health Sciences; 2013. 253-277.
11. Kumar GS. Orban's oral histology & embryology. 13th ed. *Salivary Glands*: Elsevier Health Sciences; 2011. 292-312.
12. Amano O, Mizobe K, Bando Y, Sakiyama K. Anatomy and histology of rodent and human major salivary glands-Overview of the japan salivary gland society-sponsored workshop. *Acta Histochem Cytochem*. 2012; 45(5):241–250.
13. Daniels TE, Wu AJ. Xerostomia-clinical evaluation and treatment in general practice. *J Calif Dent Assoc*. 2000;28(12):933–941.
14. Hishida S, Ozaki N, Honda T, Shigetomi T, Ueda M. Atrophy of the submandibular gland by the duct ligation and a blockade of SP receptor in rats. 2016; 78:215–227.
15. Schwarz S, Huss R, Schulz-Siegmund M, Vogel B, Brandau S, Lang S, et al. Bone marrow-derived mesenchymal stem cells migrate to healthy and damaged salivary glands following stem cell infusion. *Int J Oral Sci*. 2014;6(3):154-161.
16. Aly L, El-Menoufy H, Sadeq H, Ragae A, Sabry D. Efficiency of systemic versus intralesional bone marrow-derived stem cells in regeneration of oral mucosa after induction of formocresol induced ulcers in dogs. *Dent Res J*. 2014;11(2):212-221.
17. Okazaki H, Hattori T, Hishida S, Shigetomi T, Ueda M. Acceleration of rat salivary gland tissue repair by basic fibroblast growth factor. *Arch Oral Biol*. 2000;45(10):911–919.
18. Osailan S, Proctor G, Carpenter G, Paterson K, McGurk M. Recovery of rat submandibular salivary gland function following removal of obstruction: a sialometrical and sialochemical study. *Int J Exp Pathol*. 2006;87(6):411-423.
19. Wafaa Yahia Ibrahim Elghonamy, Olfat Mohammad Gaballah and Souzan Anwar El Amy. Effect of Platelet Rich Plasma on Regeneration of Submandibular Salivary Gland of Albino Rats. *New York Science Journal* 2018;11(12):27-40.
20. Akiyama K, You Y, Yamaza T, Chen C, Tang L, Jin Y, et al. Characterization of bone marrow-derived mesenchymal stem cells in suspension. *Stem Cell Res Ther*. 2012;3(5):40-53.
21. Shimizu O, Shiratsuchi H, Ueda K. Alteration of the actin cytoskeleton and localisation of the $\alpha 6 \beta 1$ and $\alpha 3$ integrins during regeneration of the rat submandibular gland. *Arch Oral Biol*. 2012;57(8):1127–1132.
22. Lombaert I, Wierenga P, Kok T, Kampinga H, Coppes R. Mobilization of bone marrow stem cells by granulocyte colony-stimulating factor ameliorates radiation-induced damage to salivary glands. *Clin Cancer Res*. 2006;12(6):1804–1812.
23. Cotroneo E, Proctor G, Carpenter G. Regeneration of acinar cells following ligation of rat submandibular gland retraces the embryonic-perinatal pathway of cytodifferentiation. *Differentiation*. 2010;79(2):120-130.
24. Rocchi, C.; Emmerson, E. Mouth-Watering Results: Clinical Need, Current Approaches, and Future Directions for Salivary Gland Regeneration. *Trends Mol. Med*. 2020, 26, 649–669.
25. Wang LT, Jiang SS, Ting CH, Hsu PJ, Chang CC, Sytwu HK, et al. Differentiation of Mesenchymal Stem Cells from Human Induced Pluripotent Stem Cells Results in Downregulation of c-Myc and DNA Replication Pathways with Immunomodulation Toward CD4 and CD8 Cells. *Stem Cells*. 2018;36(6):903- 14; PMID: 29396902. Available from: <https://doi.org/10.1002/stem.2795>.
26. Bulati M, Miceli V, Gallo A, Amico G, Carcione C, Pampalone M, et al. The Immunomodulatory Properties of the Human Amnion-Derived Mesenchymal Stromal/Stem Cells Are Induced by INF-g Produced by Activated Lympho-monocytes and Are Mediated by Cell-To-Cell Contact and Soluble Factors. *Frontiers in Immunology*. 2020;11(54); PMID: 32117234. Available from: <https://doi.org/10.3389/fimmu.2020.00054>.
27. Proctor G, Garrett J, Carpenter G, Ebersole LE. Salivary secretion of immunoglobulin A by submandibular glands in response to autonomic infusions in anesthetized rats. *J Neuroimmunol*. 2003;136(1):17–24.

28. Takahashi S, Nakamura S, Suzuki R, Islam N, Domon T, Yamamoto T, et al. Apoptosis and mitosis of parenchymal cells in the duct-ligated rat submandibular gland. 1998;32(6):457–463.
29. Karp J, Leng-Teo G. Mesenchymal Stem Cell Homing: The Devil Is in the Details. *Cell Stem Cell*. 2009;4(3):206–216.
30. Baxter M, Wynn R, Jowitt S, Wraith J, Leslie J, Bellantuono F. Study of Telomere Length Reveals Rapid Aging of Human Marrow Stromal Cells following In Vitro Expansion. *Stem Cell*. 2004;22(5):487–500.
31. Jones E, English A, Kinsey S, Straszynski L, Emery P, Ponchel F, et al. Optimization of a flow cytometry-based protocol for detection and phenotypic characterization of multipotent mesenchymal stromal cells from human bone marrow. *Cytom Part B Clin Cytom*. 2006;70(6):391–399.
32. Chamberlain G, Fox J, Ashton B, Middleton J. Concise review: mesenchymal stem cells: their phenotype, differentiation capacity, immunological features, and potential for homing. *Stem Cells*. 2007;25(11):2739–2749.
33. Shiba R, Hamada T, Kawakatsu K. Histochemical and electron microscopical studies on the effect of duct ligation of rat salivary glands. *Archs oral Biol*. 1972; 17:299–309.
34. Kroemer G, Galluzzi L, Vandenabeele P, Abrams J, Alnemri E, Baehrecke E, et al. Classification of Cell Death 2009. *Cell Death Differ*. 2009;16(1):3–11.
35. Walker N, Gobé G. Cell death and cell proliferation during atrophy of the rat parotid gland induced by duct obstruction. *J Pathol*. 1987;153(4):333–344.
36. Tamarin A. Submaxillary gland recovery from obstruction. Overall changes and electron microscopic alterations of granular duct cells. *J Ultrastructure Res*. 1971; 34:276–287.
37. Tamarin A. The leukocytic response in ligated rat submandibular glands. *J Oral Pathol Med*. 1979;8(5):293–304.
38. Ivanova S, Repnik U, Boji L, Petelin A, Turk V, Turk B. Chapter Nine Lysosomes in Apoptosis. *Methods Enzymol*. 2008;442(8):183–199.
39. Lodish H, Berk A, Zipursky SL, Matsudaira P, Baltimore D, Darnell J. *Molecular cell biology*. 4th edition. Natl Cent Biotechnol Information, Bookshelf. 2000; p260-270
40. Stasulis C, Hand A. Immunohistochemical identification of antigen presenting cells in rat salivary glands. *Arch Oral Biol*. 2003;48(10):691–699.
41. Harrison J, Fouad H, Garrett J. Variation in the response to ductal obstruction of feline submandibular and sublingual salivary glands and the importance of the innervation. *J Oral Pathol Med*. 2001; 30:29–34.
42. Gerlyng P, Åbyholm A, Grotmol T, Erikstein B, Huitfeldt HS, Stokke T, et al. Binucleation and polyploidization patterns in developmental and regenerative rat liver growth. *Cell Prolif*. 1993;26(6):557–565.
43. Denny P, Denny P. Dynamics of parenchymal cell division, differentiation, and apoptosis in the young adult female mouse submandibular gland. *Anat Rec*. 1999;254(3):408–417.
44. Caddick J, Kingham P, Gardiner N, Wiberg M, Terenghi G. Phenotypic and Functional Characteristics of Mesenchymal Stem Cells Differentiated Along a Schwann Cell Lineage. *Glia*. 2006; 54(8):840–849.
45. Ke X, Li Q, Xu L, Zhang Y, Li D, Ma J, et al. Netrin-1 overexpression in bone marrow mesenchymal stem cells promotes functional recovery in a rat model of peripheral nerve injury. *J Biomed Res*. 2015;29(5):380–389.
46. Sanchez-Ramos J, Song S, Cardozo-Pelaez F, Hazzi C, Stedeford T, Willing A, et al. Adult bone marrow stromal cells differentiate into neural cells in vitro. *Exp Neurol*. 2000;164(2):247–256.
47. Azizi S, Stokes D, Augelli B, DiGirolamo C, Prockop D. Engraftment and migration of human bone marrow stromal cells implanted in the brains of albino rats—similarities to astrocyte grafts. *Proc Natl Acad Sci*. 1998;95(7):3908–3913.
48. Burdon T, Paul A, Noiseux N, Prakash S, Shum-Tim D. Bone marrow stem cell-derived paracrine factors for regenerative medicine: current perspectives and therapeutic potential. *Bone Marrow Res*. 2011;2011:1-14.
49. Tran S, Liu Y, Xia D, Maria O, Khalili S, Wang R, et al. Paracrine effects of bone marrow soup restore organ function, regeneration, and repair in salivary glands damaged by irradiation. *PLoS One*. 2013;8(4):616-626
50. Fang D, Hu S, Liu Y, Quan V, Seuntjens J, Tran SD. Identification of the active components in Bone Marrow Soup: a mitigator against irradiation- injury to salivary glands. *Nat Publ Gr*. 2015;5(1):1–12.
51. Lombaert I, Wierenga P, Kok T, Kampinga H, Coppes R. Cancer Therapy : Preclinical Mobilization of Bone Marrow Stem Cells by Granulocyte Colony-Stimulating Factor Ameliorates Radiation-Induced Damage to Salivary Glands. *Clin Cancer Res*. 2006;12(24):12–15.
52. Lin C, Lee B, Liao C, Cheng W, Chang F, Chen M. Transdifferentiation of Bone Marrow Stem Cells into Acinar Cells Using a Double Chamber System. *J Formos Med Assoc*. 2007;106(1):1–7.
53. Park Y, Koh J, Kwon J, Park Y, Yang L, Cha S. Uncovering stem cell differentiation factors for salivary gland regeneration by quantitative analysis of differential proteomes. *PLoS One*. 2017;12(2):1–20.

54. Farahat M, Sathi G, Hara E, Taketa H, Kuboki T, Matsumoto T. MSCs feeder layers induce SMG self-organization and branching morphogenesis. *PLoS One*. 2017;12(4):1-14.
55. Brandau S, Jakob M, Bruderek K, Bootz F, Giebel B, Radtke S, et al. Mesenchymal Stem Cells Augment the Anti-Bacterial Activity of Neutrophil Granulocytes. *PLoS One*. 2014;9 (9):1-10.
56. Misuno K, Tran SD, Khalili S, Huang J, Liu Y, Hu S. Quantitative Analysis of Protein and Gene Expression in Salivary Glands of Sjogren's-Like Disease NOD Mice Treated by Bone Marrow Soup. *PLoS One*. 2014;9(1):1-11.

الملخص العربي

تأثير الخلايا الجذعية الوسيطة لنخاع العظم في تجديد الغدة اللعابية الموجودة تحت الفك السفلي في الفئران البيضاء

وفاء يحيى الغنيمي^١، سوزان أنور العمي^١، أميرة أحمد رزق معوض^٢، ألفت محمد جاب الله^{١،٢}

^١ قسم بيولوجيا الفم - كلية طب الأسنان - جامعة طنطا - مصر

^٢ قسم جراحة الوجه والفكين وعلوم التشخيص - كلية طب الأسنان - جامعة المجمعة - المملكة العربية السعودية

مقدمه: الغدد اللعابية هي غدد خارجية الإفراز تعمل على إفراز اللعاب ومن ثم الحفاظ على صحة الفم وبالتالي فإن انخفاض إفراز اللعاب له تأثير سلبي على صحة الفم والصحة العامة. على مدى العقود الماضية حظيت الخلايا الجذعية باهتمام كبير بسبب آثارها الناجحة في مجال الطب التجديدي

هدف البحث: دراسة التأثير العلاجي المحتمل للخلايا الجذعية المفصولة من نخاع العظم و المحقونة محليا على تجديد الغدة اللعابية الموجوده تحت الفك السفلي بعد ربط قناتها باستخدام المجهر الالكتروني النافذ

مواد و أساليب العلاج: تكونت عينة الدراسة من ٥٠ ذكراً بالغاً من الجرذان البيضاء. تم تقسيم أربعين فأراً عشوائياً إلى مجموعتين تجريبيتين متساويتين؛ المجموعة الأولى خضعت لربط قناة الغدة اللعابية الموجودة أسفل الفك السفلي خارج الفم لمدة أسبوعين وتركت دون أي علاج بعد ربط القناة، وتعرضت المجموعة الثانية لربط قناة الغدة اللعابية خارج الفم لمدة أسبوعين وتم حقنها محلياً بالخلايا الجذعية لنخاع العظم في وقت الربط. تم استخدام الفئران العشرة المتبقية لعزل الخلايا الجذعية الوسيطة لنخاع العظم. تم التضحية بخمسة فئران من كل مجموعة عند اليوم صفر، مباشرة بعد ازالة الربط، وقبل أي علاج لتقييم تأثير الربط ثم بعد ٣ و ٧ و ١٤ يوماً على التوالي. تم تخدير الفئران، وتم جمع عينات الغدة اللعابية الموجودة أسفل الفك السفلي وإعدادها للفحص بالمجهر الالكتروني النافذ

النتائج: أظهرت النتائج تغيرات تنكسية ملحوظة زادت في شدتها من اليوم صفر إلى اليوم الرابع عشر بعد ازالة الربط ومع ذلك ظهر تجديد واضح لأنسجة الغدد اللعابية التي تمت معالجتها بالخلايا الجذعية لنخاع العظم في جميع فترات المتابعة بدءاً من اليوم ٣ إلى ١٤

الاستنتاج: يؤدي ربط قناة الغدة اللعابية الموجودة أسفل الفك السفلي الى تغيرات ضمورية شديدة في أنسجة الغدد اللعابية بينما الغدد اللعابية التي تم معالجتها بالخلايا الجذعية لنخاع العظم أظهرت قدرة كبيرة على التجدد و الاستشفاء